



Low-Cost and Robust Geographic Opportunistic Routing in a Strip Topology Wireless Network

24

CHEN LIU, DINGYI FANG, XINYAN LIU, DAN XU, and XIAOJIANG CHEN,

Northwest University and Shaanxi International Research Center for Passive Internet of Things

CHIEH-JAN MIKE LIANG, Microsoft Research

BAOYING LIU and ZHANYONG TANG, Northwest University and Shaanxi International Research Center for Passive Internet of Things

Wireless sensor networks (WSNs) have been used for many long-term monitoring applications with the strip topology that is ubiquitous in the real-world deployment, such as pipeline monitoring, water quality monitoring, vehicle monitoring, and Great Wall monitoring. The efficiency of routing strategy has been playing a key role in serving such monitoring applications. In this article, we first present a robust geographic opportunistic routing (GOR) approach—Light Propagation Selection (LIPS)—that can provide a short path with low energy consumption, communication overhead, and packet loss. To overcome the complication caused by the multi-turning point structure, we propose the virtual Plane mirror (VPM) algorithm, inspired by the light propagation, which is to map the strip topology into the straight one logically. We then select partial neighbors as the candidates to avoid blindly involving all next-hop neighbors and ensure the data transmission along the correct direction. Two implementation problems of VPM—transmission spread angle and the communication range—are thoroughly analyzed based on the percolation theory. Based on the preceding candidate selection algorithms, we propose a GOR algorithm in the strip topology network. By theoretical analysis and extensive simulation, we illustrate the validity and higher transmission performance of LIPS in strip WSNs. In addition, we have proved that the length of the path in LIPS is two times the length of the shortest path via geometrical analysis. Simulation results show that the transmission success rate of our approach is 26.37% higher than the state-of-the-art approach, and the communication overhead and energy consumption rate are 33.11% and 40.23% lower, respectively.

CCS Concepts: • Networks → Sensor networks;

Additional Key Words and Phrases: WSNs, strip networks with turning points (SNWT), candidate set range, virtual plane mirror (VPM)

Downloaded from the ACM Digital Library by Xidian University on April 7, 2025.

This work was supported by the National Natural Science Foundation of China (61602382, 6157240, 61672428), the Key R&D Foundation of Shaanxi Province (2018SF-369), the International Cooperation Foundation of Shaanxi Province of China (2018KW-020), the China Postdoctoral Science Foundation (2017M623227), and the Science and Technology Innovation Team Supported Project of Shaanxi Province (2018TD-O26).

Authors' addresses: C. Liu, D. Fang, X. Liu, D. Xu, X. Chen (corresponding author), B. Liu, and Z. Tang, School of Information Science and Technology, Northwest University, No. 1 Xuefu Road, Xi'an, 710127, P.R. China, and Shaanxi International Research Center for Passive Internet of Things, Xi'an, 710127, P.R. China; emails: {liuchen, dyf}@nwu.edu.cn, 1589321878@qq.com, {xudan, xjchen, paola.liu, zytang}@nwu.edu.cn; C.-J. M. Liang, Microsoft Research, No. 5 Danling street, Beijing, P.R. China; email: liang.mike@microsoft.com.

Permission to make digital or hard copies of all or part of this work for personal or classroom use is granted without fee provided that copies are not made or distributed for profit or commercial advantage and that copies bear this notice and the full citation on the first page. Copyrights for components of this work owned by others than ACM must be honored. Abstracting with credit is permitted. To copy otherwise, or republish, to post on servers or to redistribute to lists, requires prior specific permission and/or a fee. Request permissions from permissions@acm.org.

© 2019 Association for Computing Machinery.

1550-4859/2019/03-ART24 \$15.00

<https://doi.org/10.1145/3309701>

ACM Reference format:

Chen Liu, Dingyi Fang, Xinyan Liu, Dan Xu, Xiaojiang Chen, Chieh-Jan Mike Liang, Baoying Liu, and Zhanyong Tang. 2019. Low-Cost and Robust Geographic Opportunistic Routing in a Strip Topology Wireless Network. *ACM Trans. Sen. Netw.* 15, 2, Article 24 (March 2019), 27 pages.

<https://doi.org/10.1145/3309701>

1 INTRODUCTION

Wireless sensor networks (WSNs) have been used for many long-term monitoring applications [16], such as pipeline monitoring [8, 26], water quality monitoring [19], vehicle monitoring [14], and Great Wall monitoring. A crucial requirement for the preceding applications is the reliable and real-time data transmission, which is largely determined by the routing mechanisms. Therefore, the efficiency of the routing strategy is essential in serving such monitoring applications.

It is widely received that traditional routing (TR) methods were designed with the implicit assumption of a fairly stable network topology. However, wireless multi-hop networks, such as the sensor networks and ad-hoc networks, typically have a character of unreliable link quality that causes the network topology to constantly change. For instance, a node will fail due to residual energy shortage. Hence, TR will cause packet retransmissions and communication instability, and further lead to performance degradation, such as high packet loss rate, larger energy consumption, and longer path length.

Recently, a new routing method named *opportunistic routing* (OR) [1] was proposed to reduce the effect of unreliable wireless links by utilizing the broadcasting nature and spatial diversity of the wireless medium. OR will reduce the energy expenditure related to packet retransmissions because the packet will be retransmitted only if none of the neighbors in the candidate set receives it. However, the network topology and its context information, such as the location, velocity, and timestamp, are required because a node needs to know its neighbors' information. Therefore, the current OR strategy would incur high energy and communication overhead in large-scale deployments.

In addition to OR, geographic routing (GR) [12, 13, 22] is an important research direction in the wireless network. In this case, each node can identify its own location and the source node realizes the location of the destination. With this information, the data can be sent to the sink without the global topology structure or any prior route discovery. GR can work along with OR (geographic opportunistic routing (GOR)) to reduce the energy consumption related to packet retransmissions and packet loss rate [5, 23, 29, 30]. GOR uses nodes' location information to determine the forwarding candidates and prioritize the candidates. For example, GeRaF [30] assigns higher relay priorities to candidates that are closer to the destination. GOR conserves energy and communication overhead because discovery floods and state propagation are not necessary beyond a single hop [28]. In addition, GOR also greatly reduces overhead from both computation and route establishment because neither the global knowledge of the network topology nor the routing tables are required at each node, except the location information [30]. Hence, GOR supports the stringent requirement of general resource-constraint WSNs.

However, in contrast to common belief, many strip networks with turning points (SNWT) are ubiquitous in nature, such as pipeline monitoring [8, 26], water quality monitoring [19], vehicle monitoring [14], and Great Wall monitoring (Figure 1). In such cases, GOR will cause packet loss, especially around the turning points of an SNWT. The routing hole problem occurs whenever there are no neighbors closer to the sink than itself—for instance, the current forwarding node is the closest one in the candidate set to the sink [4]. When there is no forwarding candidate

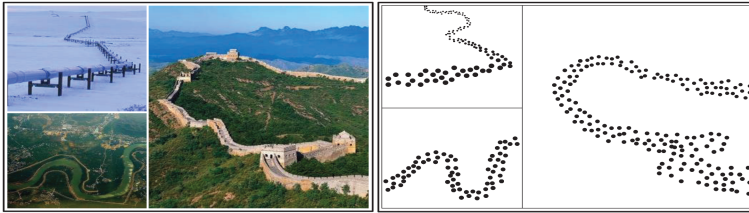


Fig. 1. Examples of the strip network in real-world deployments: pipeline monitoring, water quality monitoring, and Great Wall monitoring.

successfully receiving the packet, the sender will drop the packet after reaching the retransmission threshold. Hence, GeRaf does not have recovery mechanism to recover from routing holes.

Recently, greedy routing (GredR) methods with guaranteed delivery have already proposed to solve packet loss in the routing void region, such as GLIDER [21]. GLIDER decomposes the network into pieces such that the simple GredR can be carried out inside each piece and the adjacency of the pieces are extracted and propagated to the network on top of which global routing is performed [2]. However, it could increase the difficulty of finding the shortest path and also increase the cost of energy and latency due to the triangulation division with a high algorithm complexity. Hence, it is unrealistic for WSNs to deal with the packet loss at a high cost of both the energy and the algorithm complexity. Hence, the method adapted to the routing hole problem is unrealistic (unsuitable) for the SNWT.

To address the challenges of high latency and finding the shortest length path in the SNWT, some schemes are proposed. For example, Huang et al. [11] propose a homotopic routing scheme that generates constant bounded stretch compared to the shortest path length. Specifically, it can provide a length of the proposed greedy path that is at most $15\pi+2$ times the length of the shortest path with the low delay. However, it achieves the short path by using a coarse triangulation in the whole network, which will result in considerable energy and communication costs. Too much energy consumption will further lead to many nodes' failure. Therefore, it is unrealistic for WSNs to cope with the packet loss at a high cost of the energy.

This article introduces LLight Propagation Selection (LIPS), the low-cost and robust routing strategy based on OR and location information that works in the SNWT. In line with common practice in planning routing, LIPS broadcasts its packets to a candidate set composed of neighbors based on the location information.

Unlike the related approaches, which choose to skirt the turning points at a high cost of communication overhead, LIPS exploits a heuristic of virtual plane mirrors (VPMs) to make turning points seem to disappear (i.e., “eliminate” turning points logically to avoid packet loss caused by turnings at a low cost). Hence, the SNWT can be mapped into the straight one. To illustrate LIPS, Figure 2 shows a toy example with two turning points. The blue area is the communication range of the source. Nodes B and D are the neighbors of the source node. Node C is the neighbor of B. As the Figure shows, from the view of the spread direction of the traditional GOR, the Euclidean distance from B to the sink d_2 is shorter than the distance from D to the sink d_1 . In GeRaf [30], the source will select node B as the forwarder since d_2 is shorter than d_1 . Likewise, node B will select C as the next forwarder. Such wrong candidate selection caused by the incorrect direction will lead to transmission failure. Hence, one needs to consider the correct transmission direction in strip topology with turning points. One ignoring the transmission direction and complication of the SNWT, like the traditional based-GOR technologies, can have negative impacts. To make the source node send data in the correct transmission direction, we are inspired by the similarity between the light propagation in elementary physics and the data transmission in the network

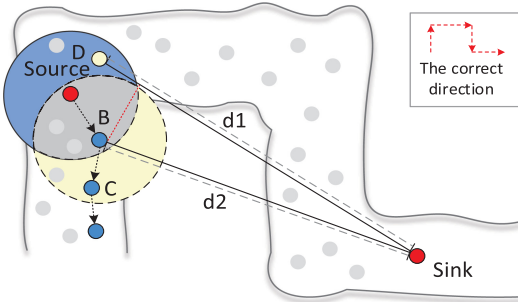


Fig. 2. The Figure shows two neighbors of the source (B and D), the neighbor of the B (C), and the sink. B, C, D represents the direction of transmission is the wrong direction.

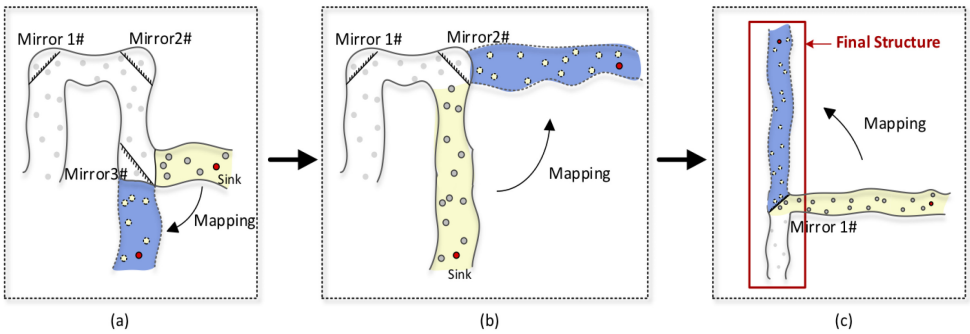


Fig. 3. The basic idea of a VPM. A VPM is located at each corner of the strip network. After multiple reflections using these virtual mirrors, the complicated strip network can be mapped into a linear one.

layer. Even if the propagate scenarios have obstacles or turning points, through the method of the plane mirror reflection, the obstacles or turning points can be eliminated in the propagation path from the logical view and the light still can propagate successfully. Hence, we employ the VPMs and use their reflection (plane mirror imaging) capability.

Our key insight is that if we consider the sink node as the point source of light, the source node as the receiver of the light (i.e., human eyes), and the turning points in the strip network as the obstacles, we can apply the principle of the light reflection by a plane mirror to guide the data transmission in the strip network. To do this, we propose the VPM algorithm (Section 4), where a VPM (i.e., a linear equation) is positioned in the center of each turning region to map the whole strip structure into a linear structure by all VPMs step by step. To illustrate the VPM algorithm, Figure 3 shows a toy example with three turning points, where three virtual mirrors (three linear equations) are located in the center of each turning points and the sink node is deployed behind the third turning point. As Figure 3(a) shows, the nodes within the yellow subregion can be mapped to their virtual images based on Mirror 3#. Similarly, after three times mapping (Mirror 3#, Mirror 2#, and Mirror 1#), the complicated strip structure with three turning points can be mapped into a linear structure (see Figure 3). Figure 4 shows the linear topology network via the VPM's mapping transformation using the VPM. It is clear from this Figure that looking at the strip structure alone, the original structure would wrongly indicate that B is the forwarder, whereas looking at the mapped (straight) structure allow us to realize that B is far away from the sink and that D is the correct forwarder. It is obvious that the blue region definitely does not have the forwarder if the yellow region already has the node in GOR-based technologies. It can be seen that blindly

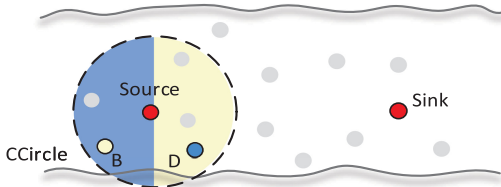


Fig. 4. Mapped structure via the VPM. The Figure shows a source node and a sink; CCircle represents the source communication range.

including (involving) all the available neighbors into the candidate set is unnecessary. Thus, the key challenge for a robust routing scheme is selecting the proper candidate set, by quantifying the range of candidate set.

So how can we determine the range of candidate sets for the mapped straight topology? To do so, we need to consider the communication range and the distance from the source to the sink. In contrast to the preceding illustrative example, real-world deployments' topology always changes owing to the complex and volatile environment. Further, the forwarding candidate set is changed depending on the changed topology. In designing a method that selects the candidate set range despite these variations, we are inspired by the spread of the point-source light propagation. There especially is an angle between the two lines from the source point to the human eye. If we can make the sink as the source point and the source as the human eye, the range of the source to the sink must have an angle. Therefore, we take this angle to determine the range of the candidate set. However, if the angle is too small, like 0.01π , maybe there are no neighbors in the range, which will cause the packet loss. If it is too large, as mentioned earlier, such as 2π degree, maybe there are too many neighbors involved in the range, which causes unnecessary communication overhead and reception energy consumption.

Finally, we make a deep analysis of the spread angle to ensure proper range. To this end, we determine the threshold of spread angle via the percolation theory. In addition, we prove that the routing length of the proposed VPM algorithm is at most two times the length of the shortest path.

Summary of results. We built a strategy of LIPS and evaluated it with a deployment in Shibadun, a part of the Great Wall that lies in Yulin, Shaanxi, China (shown later in Figure 14). We compare LIPS's performance in routing with state-of-the-art GOR and GredR-based methods, described in Section 6. LIPS and compared strategies all use the same topology and sensor nodes. Our experiments lead to the following findings:

- Compared to the classic algorithm, LIPS improves the transmission success rate and reduces both the communication overhead and energy consumption in the strip WSNs. Furthermore, it can provide a constant bounded stretch compared to the shortest path length.
- In the non-strip networks, the LIPS's transmission success rate and energy efficiency are still higher than the classical algorithm, such as traditional GOR.

Contributions. This work makes the following contributions:

- It presents the robust routing strategy that exploits transmission direction as a major concern of the data transmission. As a result, the design delivers the high transmission success rate, low energy cost, and a shorter path even in the strip topology network.
- It is also the first to demonstrate the capability of using the VPM to map the strip topology network to the straight one. Although the design and results are demonstrated in the context of strip WSNs, the basic idea can be extended to other wireless networks. It is also the first to utilize the spread angle to identify the forwarding candidate set.

- It presents a solution, far less than the previous method, that the length of the VPM path is at most two times the length of the shortest path.
- It has been demonstrated that it not only can it be used in the strip topology but it also obtains better performance than GOR-based techniques in the regular shape network.

2 RELATED WORK

Early efforts on routing protocols in WSNs focus on energy-efficient and reliable transmission mechanisms. Typically, in energy-aware routing (EAR) [24], the path is predefined by mainly taking the energy into account, and the goal is to prolong the network lifetime. EAR-based techniques, however, may result in many data retransmissions under unreliable communication links. Furthermore, for the large-scale strip networks, the predetermined node may fail in harsh environments of rain or snowstorms, which reduce the transmission success rate. Hence, EAR will cause packet loss and further increase the communication overhead.

There is a growing interest in using GredR with guaranteed delivery to avoid the packet loss. The study of Huang et al. [11] provides a greedy path that is at most $15\pi + 2$ times the length of the shortest path with low delay. However, it achieves the short path by using a coarse triangulation in the whole network, which will result in high algorithm complexity of considerable energy and communication costs during the routing procedure. Hence, GredR-based techniques are less practical for the multi-turning strip structure. It remains a major challenge for these techniques to address the excessive energy consumption and the path length in the SNWT.

Researchers have also investigated the possibility of using OR to improve the transmission reliability by utilizing the broadcast nature and the spatial diversity of the wireless medium, which reduces the packet loss obviously. Specifically, OR does not specify a single path to transmit packets in advance. In contrast, OR adopts the broadcast method to send the message to all neighbors and select one with the highest priority to forward the packet. However, topological knowledge is required because a node needs to know its neighbors' information. Hence, OR will cause a significant communication overhead.

GOR is a type of OR based on location information. GOR largely reduces the communication overhead and the energy consumption since it eliminates the requirement of establishing complete routes to the destinations. Additionally, the routing messages that update the routing path state are no longer necessary. Further, GOR also faces another main problem: the packet loss in the communication void region where there exists no adjacent node that is closer to the sink than a forwarder node—for instance, the current forwarder node is the closest one to the destination [4], such as turning points. In such a case, a heuristic mapping that uses the VPM to map the strip structure to a straight one should be considered. By doing this, the communication void region (i.e., turning points) seems to virtually disappear, and thus it can reduce the packet loss.

In the context of routing protocol, the approaches in Zorzi and Rao [30], such as GeRaF, use GOR-based methods and the concept of the candidate set to improve transmission reliability. Although LIPS also utilizes the concept of the candidate set, it significantly differs from all related approaches in the number of the candidates. Past schemes blindly ignore the transmission direction and involve all the available next-hop neighbors as the forwarding candidates at a cost of high overhead [28]. In contrast, LIPS systematically reduces the number of forwarding candidates and selects the subset of the candidate set in the correct transmission direction, which reduces the energy cost and the communication overhead. The synergy between the mapping method and the range of the candidate set enables LIPS to forward the packet via multiple hops from the source to the sink successfully. This approach enables the routing strategy in scenarios with SNWT at the low energy cost and packet loss.

LIPS is related to a wide range of works in monitoring application. Most of these systems are based on GredR strategies to transmit the data, whereas some use the GOR strategies. In particular, the work in Zorzi and Rao [30] uses a candidate set involving all neighbors to select the highest-priority node as the next hop forwarder so as to avoid the link unreliability of a single path. Although LIPS also uses a candidate set concept, it employs a partial candidate set and selects forwarding candidates using a proper spread angle to enable low communication overhead and energy consumption. Further, LIPS's solution to the turning points is different: past methods ignore the importance of correct transmission direction in the turning points and get stuck when there are no neighbors who are the closest node to the sink than itself. LIPS considers the correct transmission direction to map the strip topology into the simple straight topology logically, which allows it to achieve a significantly higher transmission success rate. Additionally, recently a few routing protocols [10] have proposed to solve the strip topology problem. Compared to these mechanisms, LIPS differentiates itself in objectives, techniques, and operating environments. LIPS's objective is to transmit data in SNWT, which by nature are employed in the multi-turning points region and violent environments. To do so, LIPS exploits the mapping method as opposed to the direct greedy forwarding.

In addition, a few recent proposals in the data fusion field apply the angle transmission from collectors to the mobile sink when the collectors gather enough data [7]. LIPS's use of the angle differs in that it is based on the candidate set, of which we select the proper subset.

For the edge identification of the monitoring area, in Tan et al. [27], the authors proposed a distributed convex partitioning protocol for large-scale WSNs with complex topologies. In Liu et al. [17], they set up a skeleton node to form a skeleton in the 2D/3D sensor network to keep the routing unobstructed. The method proposed in Liu et al. [18] divided the network into several convex parts, and the authors set up a virtual coordinate system to label the region. Inspired by this work, we apply their convex division method and extend it to the strip network to obtain the width, length, and turning points of the strip structure in the initial stage of LIPS.

3 LIPS OVERVIEW

3.1 Overview

LIPS is a low-energy and high transmission success rate GOR strategy for the strip topology network, and the proved path length is at most two times the length of the shortest path compared to the classic algorithm. Following a common practice in routing strategies, LIPS leverages the most commonly used Z-Stack motes to deploy a set of sensor nodes in the environment. LIPS first identifies the width, the length, the turning points, and each turning's angle of the strip network using the existing method [18]. This means that we can obtain the locations of each virtual plane mirror, and the values of the key parameters in LIPS, such as the radius R , the nodes communication range r , and the distance from the source to the sink d . More specifically, these values and the strip structure information are stored in each node. Furthermore, each node knows the location information of its own and its neighbors. In addition, the destination (the sink) location is also known to each node.

To monitor an SNWT at a high level, LIPS goes through the following steps, as Figure 5 shows:

- *Identify the boundary of the strip structure.* LIPS applied the curvature detection algorithm proposed in Liu et al. [18] to identify a boundary node, then based on the relative locations between these boundary nodes, LIPS established the relative coordinate for each node in the monitoring area. Finally, the width, length, and turning points of the stripe can be identified correctly based on the relative coordinate (Section 4.1).

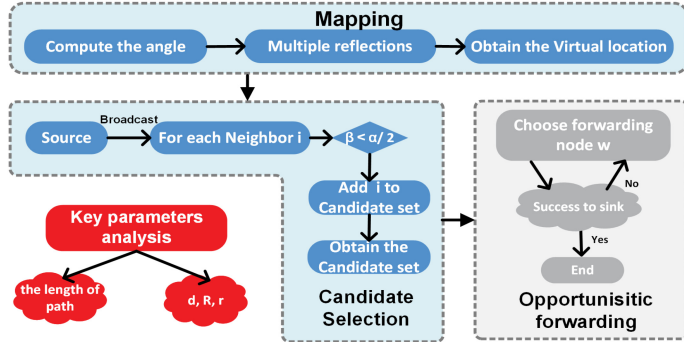


Fig. 5. An overview of LIPS.

- *Mapping.* LIPS computes the angle of each VPM through such known information (i.e., the width, length, and turning-point angle). Then, LIPS can obtain the virtual location of each node by multiple reflections using mapping matrices. Namely, LIPS makes the SNWT mapped to the straight one in Section 4.
- *Candidate selection.* By calculating the communication range and the radius R , as well as the distance between the source and the sink, LIPS can identify the range of spread angle α for the subcandidate set in Section 4. Specifically, a source node broadcasts the packet to each neighbor, then the neighbor nodes judge whether or not they are within the spread angle α . For simplicity, we denote the neighbor angle β_i as the angle formed by the sink, the source, and its neighbor node i . If the condition $\beta_i < \alpha/2$ holds, the neighbor i will be added to the candidate set.
- *OR.* In the routing phase, according to the candidate selection, the source node selects the forwarder from the candidate set by considering the node residual energy, the distance from the source to the sink, and the link quality via OR.
- *Key parameters analysis.* In large-scale deployments like the Great Wall monitoring and underground Port Road monitoring, there can be a large number of sensor nodes. It is essential to choose the proper spread angle to decrease the communication cost. We make a theoretical analysis on the range of the key parameters (i.e., the communication range r , the radius R , and the distance d from the source to the sink) and prove their thresholds in Section 5.

The next few sections elaborate on the preceding steps, providing the technical details. The notations used in the article are shown in Table 1.

4 CANDIDATES SELECTION IN LIPS

The candidate selection in a routing strategy is a procedure of broadcasting the packet to neighbors and selecting one neighbor to forward data according to the priority. However, the nature of the SNWT will increase the difficulty of selecting the correct forwarding node. Hence, in this section, we focus on how to “eliminate” the turning points from the logical view and select the proper and correct candidate set.

In traditional GOR, the node selects all the neighbors within its one-hop range as the candidate forwarders and assigns higher relay priorities to forwarders that are closer to the destination. However, such an approach would cause packet loss and significant energy consumption because of the difficulty of finding the shortest path length in strip topology with turning points. Thus, it cannot be adopted directly. Alternatively, if we can make the complicated strip network topology map to a simple topology (i.e., straight topology), we can take the preceding method to forward

Table 1. List of Notations

Symbols	Definition
The radius R	The Euclidean distance between the sink and its arbitrary neighbor node u .
r	The communication range of nodes.
d	The distance from the source to the sink.
The spread angle α	The angle formed by the source and two tangents to the image of LCircle.
The neighbor angle β	The angle formed by the sink, the source, and its neighbor node.
The turning angle θ_m	The angle of the turning region. It describes the curvature of the turning point m .
The angle η_m	The angle between the plane mirror m and the horizontal direction.
CCircle	The one-hop range of the source node.
LCircle	This circle presents the “light area” of the sink with the radius R .

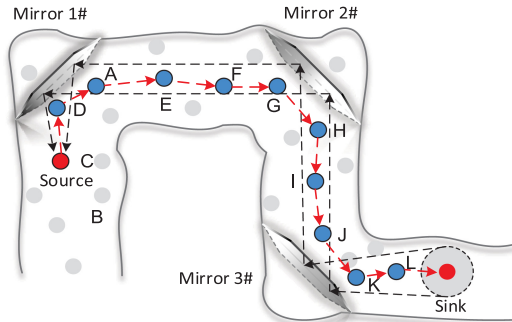


Fig. 6. Illustration of the VPM algorithm showing the transmission path via multiple reflections from source to sink with the aid of two reflected rays. The forwarding path to the sink via the mapping method can be determined with “DAEFGHIJKL,” where the “D”, “A”, “E”, “F”, “G”, “H”, “I”, “J”, “K”, “L” is the forwarding sensor node.

the packet. To make the strip topology mapped into the straight one, we need to make turnings seem to disappear (i.e., eliminate the turning points). We proposed a heuristic that the obstacles or turning points can be eliminated through the method of the plane mirror reflection in the transmission path from logical view. For instance, submarine personnel often observe the activities of the surface through the periscope’s two reflections. Hence, we propose the VPM algorithm to make the complicated multi-turning points region mapped into the simple straight one. When mapping transformation is accomplished, to reduce the cost, we have to consider the proper range of the candidate set. We choose a spread angle α to address the candidate set range, and then the region of the candidate set can be limited in a sector.

To visually understand this idea, let us again consider the simple setup shown in Figure 2. Figure 6 shows the transmission path by considering the transmission direction by utilizing the VPM’s reflection principle. Each sensor node stores the location information of its own and its neighbors, and the VPM location and the sink location as well. Through the way of the VPM combined with the range of candidate set, we can obtain a definite transmission direction. When the source decides whether to forward packet to its neighbor node B or to the neighbor node D , the combined mechanism can tell the node to forward to D , thereby avoiding the routing void in

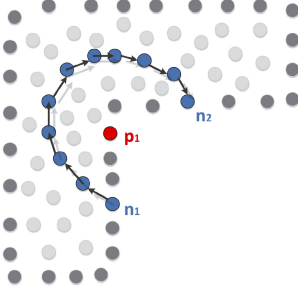


Fig. 7. Approximate convex decomposition method.

the turning points (B is the nearest node to the sink from Euclidean distance, and D is the nearest node to the sink along the strip network). Similarly, the sensor node D chooses its neighbor A rather than other nodes. Figure 6 shows the fact that the source can transmit the message to sink successfully via the VPM algorithm.

4.1 Identify the Boundary Nodes

In the real-world deployment, the width, length, and turning points of the monitoring area are unknown in the initial stage. To solve this problem, we use the approximate convex decomposition [18] method to identify the boundary node. Then we use the curvature to calculate whether a boundary node is a concave node or not. As shown in Figure 7, suppose that n_1 and n_2 are two random nodes in the strip monitoring area. The node P_1 is on the same boundary with nodes n_1 and n_2 . Thus, the k-hop curvature of $\text{arc}(n_1n_2)$ can be calculated by

$$C_k(n) = \frac{|d_k^n(n_1, n_2)|}{k \times \pi}, \quad (1)$$

where $d_k^n(n_1, n_2)$ denotes a perimeter from n_1 to n_2 . If $C_k(n)$ is larger than a given threshold (we use the threshold in Dong et al. [3] for identifying the boundary node), we will consider node n as a concave node. After several iterations, we can select the boundary nodes of the strip structure.

According to the relative locations between the adjacent nodes, we establish the relative coordinate of every node as follows:

$$(x_i, y_i) = (x_i - a, y_i - b), \quad (2)$$

where (x_i, y_i) is the coordinate of an arbitrary node and (a, b) is the abscissa and ordinate of the first boundary node in this area. According to the relative coordinate, the width, length, and turning points of the stripe can be obtained.

4.2 VPM Algorithm

In designing the VPM algorithm for mapping the strip structure into a straight one, we are inspired by the light propagation problem in elementary physics. It is understandable that even if the propagation scenarios have obstacles or turning points, the light may propagate straightly (successfully) accordingly to the reflection.

Our key insight is as follows. If we consider the sink node as the point source of light, the source node as the receiver of the light (i.e., human eyes), and the turning points in the strip network as the obstacles in the light propagation, then by using the reflection of the plane mirror, the source node can “see” the virtual image of sink behind the mirror directly, as shown in Figure 8. Then the transmission path from source to sink is similar to the reverse light propagation path the human eye receives from the light source. Thus, the source node can find the reverse light path in certain

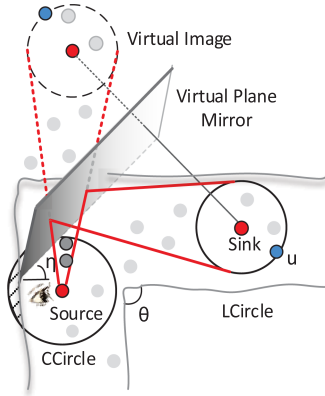


Fig. 8. A detailed reflection at one turning point. The source can “see” the sink image behind the mirror via the reflection.

spread angle α to the sink node using the plane mirror reflection principle, which can ensure that the transmission path along the network keeps consistent with the direction of transmission. In this way, the complicated turning points seem to disappear and the transmission direction can be determined on a correct angle. Having recognized the similar nature of VPM’s mapping of the strip structure into a straight one and the reflection of light propagation, we borrow the idea from light propagation. Thus, we propose a VPM algorithm to address this problem.

4.2.1 Mapping. To eliminate the turning point from the visual and select the correct candidates to ensure the correct transmission direction, inspired by the light propagation, we propose a mapping method. In this approach, the SNWT can be mapped into a straight network topology from a logical view by multiple reflections. In VPM, a VPM is positioned in the center of each turning region. Suppose that the total number of mirrors is M for a given strip structure. According to the plane mirror reflection principle, the angle η_m between the plane mirror m and the horizontal direction should keep consistent with the turning angle θ_m in the turning point m . The angle η_m is computed by

$$\eta_m = \pi/2 - \theta_m/2, \quad (3)$$

where the angle η_m of the VPM m is defined that the angle between the plane mirror and the horizontal direction, and where the θ_m is the angle of the turning point m .

For the complicated turning strip network (shown in Figure 6), we provide one VPM in each turning point, and thus the source node will “see” the sink node easily with multiple reflections in a similar manner as human eyes can see the source of light with multiple reflections. More specifically, the whole strip structure can be mapped to a straight structure by all virtual plane mirrors step by step. For an arbitrary node w , assume that it is behind the m^{th} mirror, and thus its location (x_w, y_w) can be mapped to virtual location (x'_w, y'_w) :

$$\begin{bmatrix} x'_w \\ y'_w \end{bmatrix} = T_{m+1} \times T_m \times \cdots \times T_1 \times \begin{bmatrix} x_w \\ y_w \end{bmatrix}, \quad 0 < m < M, \quad (4)$$

where M and m are the total numbers of VPMs and the sequence of the VPM, respectively. T_{m+1}, T_m, \dots, T_1 are the mapping matrices of each VPM. From the principle of the reflection, the preceding mapping matrix is the rotation matrix in Equation (5).

$$T_m = \begin{bmatrix} \cos(2\eta_m) & -\sin(2\eta_m) \\ \sin(2\eta_m) & \cos(2\eta_m) \end{bmatrix} \quad (5)$$

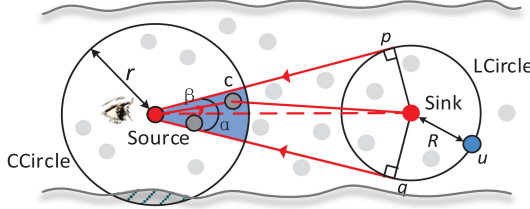


Fig. 9. Candidate selection. The Figure shows the straight network topology from Figure 8 mapping.

Therefore, Equation (4) can be converted to

$$\begin{bmatrix} x'_w \\ y'_w \end{bmatrix} = \begin{bmatrix} \cos(2\eta_{m+1}) & -\sin(2\eta_{m+1}) \\ \sin(2\eta_{m+1}) & \cos(2\eta_{m+1}) \end{bmatrix} \times \dots \times \begin{bmatrix} \cos(2\eta_1) & -\sin(2\eta_1) \\ \sin(2\eta_1) & \cos(2\eta_1) \end{bmatrix} \times \begin{bmatrix} x_w \\ y_w \end{bmatrix}, 0 < m < M. \quad (6)$$

If $m = M$, its virtual location is

$$\begin{bmatrix} x'_w \\ y'_w \end{bmatrix} = \begin{bmatrix} x_w \\ y_w \end{bmatrix}. \quad (7)$$

Let us use the example in Figure 8 to illustrate the VPM algorithm in each turning region in more detail. Assume that the turning angle $\theta = 90^\circ$, a mirror is located at the center of the corner with an angle $\eta = 45^\circ$. The sink selects a node u within its one hop, and a circle is formed with center sink and radius R , where R is the Euclidean distance between node u and the sink. This circle presents the “light area” of the sink and is defined as LCircle. We will confirm the range of R by analysis and simulations in the following section. A circle referred to as CCircle is the one-hop range of the source node, and all the nodes within the CCircle can be seen as the possible candidates.

4.2.2 Candidate Set Range. After mapping, virtual images can construct a straight region shown in Figure 9. Accordingly, the complicated SNWT can be simplified. Then we have to consider the number of the neighbor nodes in the candidate set. In practice, it is energy wasting to broadcast the packet to all next-hop neighbors and even can shorten the global network lifetime. Inspired by the point source of light propagation, we use partial candidates set to select the forwarding candidate.

The detailed mapping is given by Figure 8, where the virtual images of the sink node and its LCircle are shown behind the virtual mirror. Then we make two tangents to the virtual LCircle from the source node and obtain two reflection rays. According to the incident point, it can easily obtain two incident rays. Thus, the candidates’ area is constructed by two incident rays, two reflection rays, a virtual mirror, and the CCircle. We define the spread angle as the angle formed by the source and two tangents to the image of LCircle.

To ensure a short path length and reduce the costs of both the energy and the communication, the region included by the spread angle α indicates the path to the sink node. Namely, for arbitrary node c in CCircle, if the conditions $\beta < \alpha/2$ holds, then node c can be added to the forwarding candidates. Here, β and $\alpha/2$ can be computed by law of cosines and law of sines, respectively. Therefore, the condition can be regarded as

$$\arccos \frac{d_{sc}^2 + d^2 - d_{csink}^2}{2 \times d_{sc} \times d} < \arcsin \frac{R}{d}, \quad (8)$$

where d_{sc} is the distance between node c and node s , d is the distance between node s and the sink, and d_{csink} is the distance between node c and the sink. R is the radius and r is the communication range of nodes.

For example, a specific sender transmits the packet that contains its own location information. Then, its next-hop neighbors receive this packet and calculate the above condition defined in Equation (8). All the nodes within the transmission direction belong to the forwarding candidate set. The VPM algorithm can be summarized as Algorithm 1.

To avoid the situation where the packet goes further than the sink, we marked the nodes that are within one hop of the sink as *neighbor-sink* in the initial stage. When the *neighbor-sink* node receives the packet, it directly forwards the packet to the sink and stops the candidate selection procedure.

4.3 OR Strategy

After we pick the candidate set with VPM, we will need to select an appropriate sensor node as a forwarder to relay the communication packet. To do so, we assign a priority to each forwarding candidate based on its distance to the sink node, the residual energy, and the reliability of the link—for instance, a node that is closer to the sink node and has more energy and higher link quality is likely to be chosen as a forwarder. Thus, we choose the candidate that has the high priority as the preferred forwarder. If there is a transmission failure, we will choose the subprime candidate to forward the message until it arrives at the sink. To reduce the number of replicated messages, not all forwarding candidates will relay the message. Instead, a candidate only forwards the message that is not been forwarded by other candidates. The priority is calculated as follows:

$$P_{w\text{-}send} = \omega_e \times \frac{e_w}{E_{min}} + \omega_d \times \frac{D_{max} - d_w}{D_{max}} + \omega_L \times \frac{Q_w}{Q_{min}}, \quad (9)$$

where $P_{w\text{-}send}$ is the forwarding priority of an arbitrary node w , and ω_e , ω_d , and ω_L are the weights of the energy, the distance, and the reliability, respectively ($\omega_e + \omega_d + \omega_L = 1$). The current residual energy, the link reliability, and the distance to the sink are denoted as e_w , Q_w , and d_w . E_{min} refers to the minimum energy of an arbitrary node to alive, D_{max} is the maximum distance from an arbitrary node to the sink in the monitoring area, and Q_{min} is the minimum link quality indicator for a successful transmission.

To handle the situation when the connectivity around the mirror is lost, LIPS will select the top-k high priorities and randomly choose one among them as the forwarder. In this case, we can balance the energy consumptions among different nodes. In addition, we can add some nodes around the mirrors as the backup to handle this problem. Although this will increase the costs of the hardware, the number of turning points in the strip structure is greatly smaller than the total number of deployed nodes. In other words, the number of backup nodes is reasonable. For the more complicated scenarios and the corresponding solutions, we leave it to our future work.

Furthermore, we introduce the LIPS_modify algorithm as a baseline to compare to LIPS, which constantly chooses a node randomly in the candidates set as the high priority to forward data, until the data is forwarded successfully.

5 A DEEP ANALYSIS ON THE RANGE OF KEY PARAMETERS IN LIPS

To understand LIPS deeply, in this section we first analyze how LIPS generates constant bounded stretch compared to the shortest path. Then we theoretically derive the threshold of the spread angle α and communication range r to ensure a non-empty forwarding candidate set, which is also verified by simulation results.

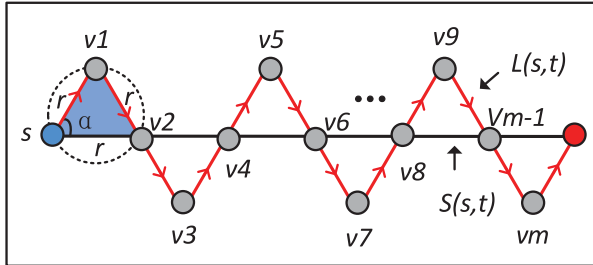


Fig. 10. The length of the path in LIPS Algorithm.

ALGORITHM 1: VPM Algorithm.**Input:**The strip network, N_{strip} ;The parameters, R, r ;**Output:**The forwarding candidates set, $Candidates$;

- 1: Map the complicated turning strip network into a straight network and obtain the virtual locations of each node (X', Y');
- 2: Select a source node randomly to send data packet;
- 3: Source node broadcasts the data packet;
- 4: Its neighbors calculate whether they are within the transmission angle using Equation (8);
- 5: Add the neighbors that are within the angle to the Candidates set;
- 6: **return** $Candidates$;

5.1 The Analysis on the Length of the Path in LIPS

THEOREM 5.1. *Given a strip topology network with turning points, LIPS finds a path of length at most two times the length of the shortest path following the same source and the destination.*

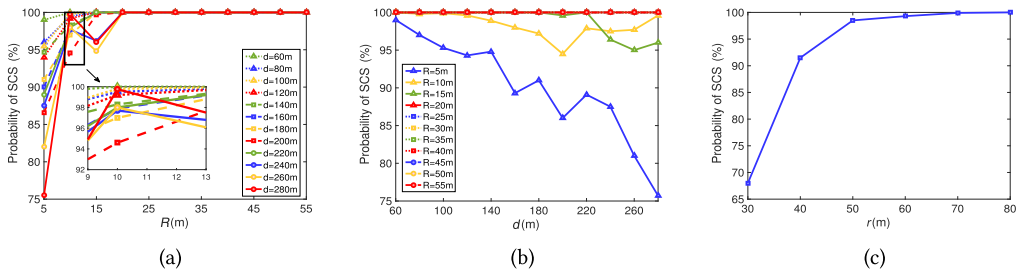
PROOF. For the source node s and the destination t , we use $|L_{s,t}|$ to denote its path length and $|st|$ to denote the Euclidean distance between s and t . Let us represent the LIPS algorithm path by $P_{s,t}$ and the shortest path by $S_{s,t}$.

Since an arbitrary strip structure can be mapped to the straight structure by all VPMs, the shortest path from s to t is a straight line along the straight structure. Thus, the length of the shortest path $S_{s,t}$ is the Euclidean distance $|st|$ (e.g., $|L_{S_{s,t}}| = |st|$).

As shown in Figure 10, the worst case of LIPS is that it chooses the farthest node within the spread angle α for each hop. Thus, the path is a fold line along the line of sight (LOS) between s and t . For example, s chooses v_1 , which is the farthest one within angle α as the forwarder. v_1 chooses v_2 as the next forwarder, and v_2 is just not in the communication range of s . Thus, the triangle formed by s , v_1 , and v_2 is an equilateral triangle. Similarly, all the equilateral triangles consist of the whole path. It is obvious that the length of the fold line is two times the length of the Euclidean distance between s and t . For example,

$$|L_{P_{s,t}}| = 2|st|. \quad (10)$$

In other words, $P_{s,t}$ is two times of the shortest path $S_{s,t}$. □

Fig. 11. The impact of R , d , and r on the VPM algorithm.

5.2 The Impact of the Spread Angle α and the Communication Range

In this section, we analyze the following three points to see how LIPS achieves good performance: (i) the impact of spread angle α to the candidates selection; (ii) the impact of r to the candidates selection; and (iii) the bounds for the critical thresholds of R , d , and r .

5.2.1 Empirical Study and Observations. Before presenting the analytical results, let us first obtain a number of insights from simulation studies.

- (*The impact of radius R of LCircle on the VPM algorithm*). First, we simulated a complicated strip network and mapped it into a straight network with a length $L = 600m$, a width $b = 30m$, and communicating range $r = 60m$. $N = 400$ sensor nodes are randomly deployed in the region. The distance d between the source node to sink is changed between 60m and 280m with the step 20m and R is changed between 5m and 55m with the step 5m. We evaluate more than 1,000 runs. For each time, we select a node as the source node randomly to send a data packet to sink. More conveniently, if the candidate set is not empty of a sending node when using VPM, we denote this situation as *successful selection*. The probability of successful selection via the VPM algorithm for some specific values of R is plotted in Figure 11(a). We observe that there is a critical threshold of R that depends on d for a given r , at which there appears a rapid increase in the probability of successful selection. Note that such a probability is close to one, when d is smaller than 180m, but it is much larger than the width of b . In addition, when R is larger than 20m, the probability is close to one no matter what the value of d is. In our solutions, we set $R = 20$ and pre-stored it in each node.
- (*The impact of distance d between the source node to sink on the VPM algorithm*). Using the same set of simulations, we evaluate the distance between the sender and sink node d . The results are shown in Figure 11(b). We observe that there is a critical threshold of d that depends on R for a given r , at which the probability of successful selection is close to one. The probability is decreasing as d is increasing when $R = 5m$, but it is close to one no matter what value d is when R is larger than 20m. This is not surprising, as it suggests that the successful candidates selection in strip network depend on both R and d . Actually, the spread angle depends on both R and d , as $\sin \alpha/2 = \frac{R}{d}$. These two factors indicate that there is a critical threshold for spread angle α in candidates selection. Note that such a probability is close to one when R is sufficiently larger than 20m but is smaller than r .
- (*The impact of communication range r on the VPM algorithm*). We also evaluate the communication range r to the probability of successful selection for a given $R = 20m$ and $d = 140m$, as shown in Figure 11(c). Note that the successful selection indicates the reachability from an arbitrary node to the sink. We observe a similar phenomenon as R and d analyzed earlier.

There do exist a critical threshold of r . Namely, when r is larger than 50m, the probability is close to one.

5.2.2 Theoretical Analysis. The results of the preceding empirical studies are useful to certain optimization problems subject to successful candidate selection. In light of the percolation theory, we derive bounds for the critical threshold of spread angle α in a strip network for a given r . We focus on the case $0 < \alpha < \pi$. Similarly, we also derive that of r for a given α . The node deployment of the strip network is modeled as a 2D Poisson point process, and thus the optimal candidates selections with the limitation of forwarding directions study is to map the Poisson point process with directional transmission to a site percolation model [2].

Let the percolation probability for site percolation model at link probability p be (see Chau et al. [2]):

$$\theta_{dir}^{*sp}(p) \doteq P\{v_o \leftrightarrow \infty\}, \quad (11)$$

where $p = 1 - e^{-A}$ and A is the cell area, and $\{v_o \leftrightarrow \infty\}$ denotes the event that there exists an infinite long undirected path starting at the center v_o . The critical threshold of p is defined by

$$P_{dir}^{*sp} \doteq \inf\{p \geq 0 : \theta_{dir}^{*sp}(p) > 0\}. \quad (12)$$

THEOREM 5.2. (See [6, 15, 20]) *The critical thresholds are bounded by*

$$\frac{2}{3} \leq P_{dir}^{*sp} \leq \frac{3}{4}. \quad (13)$$

Denote the percolation probability for a Poisson point process with the directional transmission in a strip network by $\theta_{po}^{stsp}(R, d, r)$ and the critical thresholds of R , d , and r that induce percolation as

$$\begin{aligned} R_c^{stsp}(d, r) &\doteq \inf \left\{ 0 < \frac{R}{d} < 1, 0 < R < r : \theta_{po}^{stsp}(R, d, r) > 0 \right\}, \\ d_c^{stsp}(R, r) &\doteq \inf \left\{ 0 < R < r : \theta_{po}^{stsp}(R, d, r) > 0 \right\}, \\ r_c^{stsp}(d, R) &\doteq \inf \left\{ d > 0, 0 < R < r : \theta_{po}^{stsp}(R, d, r) > 0 \right\}. \end{aligned} \quad (14)$$

The fundamental thought is that a Poisson point process with directional transmission can be solved with a site percolation model.

Hence, it can apply Theorem 2. Here, two mappings are introduced, DL and DU [2]. They represent the two kinds of directed site percolation models shown in Figure 12(a) and (b) that allow us to use the upper and lower bounds, respectively, from Theorem 2.

DU is defined by a cell with a sector of angle α and radius $r/2$, as shown in Figure 12(a). The cells are placed in the region of Poisson point process. Nodes that are lying outside cells can be ignored. For DL, it is defined by a cell with a rectangle of width r , as shown in Figure 12(b).

THEOREM 5.3. *The critical thresholds for a strip network are bounded by*

$$\begin{aligned} \sqrt{\frac{d^2}{1 + \frac{4r^4}{\log 3^2}}} &\leq R_c^{stsp}(d, r) \leq \min \left\{ r, d \times \sin \frac{4\log 4}{r^2} \right\}, \\ \frac{R}{\sin \frac{4\log 4}{r^2}} &\leq d_c^{stsp}(R, r) \leq \sqrt{\frac{4r^4 R^2}{\log 3^2} + R^2}, \\ \sqrt{\frac{\log 3 \sqrt{d^2 - R^2}}{2R}} &\leq r_c^{stsp}(d, R) \leq 2 \sqrt{\frac{\log 4}{\arcsin \frac{R}{d}}}. \end{aligned} \quad (15)$$

PROOF. The upper bounds of r , R and the lower bound of d are built by mapping DU, whereas the lower bounds of r , R and the upper bound of d are established by mapping DL. In DU, we note that in a pair of neighboring cells the distance between a pair of nodes is at most r . Hence, if a pair of neighboring sites (blue circle shown in Figure 12(a)) is enabled, then there exists a pair of nodes individually lying in the respective cells that are connected by directional transmission with spread angle α and range r . In other words, the connectivity of the directed lattice suggests the node connectivity with the directed transmission. Thus, we obtain

$$\theta_{dir}^{stp}(p) \leq \theta_{po}^{stp}(R, d, r), \quad (16)$$

where $p = 1 - e^{-A}$ and $A = \frac{\alpha(r/2)^2}{2} = \frac{2 \arcsin \frac{R}{d} \times (r/2)^2}{2}$ is the cell area. By Theorem 2, there exists $p = p_c^{sp} \leq \frac{3}{4}$, and therefore we obtain $1 - e^{-A} \leq \frac{3}{4} \Rightarrow$

$$\begin{aligned} R_c^{stp}(d, r) &\leq \min \left\{ r, d \times \sin \frac{4 \log 4}{r^2} \right\}, \\ d_c^{stp}(R, r) &\geq \frac{R}{\sin \frac{4 \log 4}{r^2}}, \\ r_c^{stp}(d, R) &\leq 2 \sqrt{\frac{\log 4}{\arcsin \frac{R}{d}}}. \end{aligned} \quad (17)$$

In DL, we found it impossible to connect a pair of nodes in different cells separated by more than one level with directional transmission. Therefore, there does not exist a connected nodes sequence in the respective cells with spread angle α and range r if there is not a connected sequence can make the site in the lattice via directed links. In other words, the disconnectivity of directed lattice suggests the disconnectivity of nodes with directed transmission. Thus,

$$\theta_{dir}^{stp}(p) \geq \theta_{po}^{stp}(R, d, r), \quad (18)$$

where $p = 1 - e^{-A}$ and $A = 2r^2 \tan \alpha / 2 = \frac{2r^2 R}{\sqrt{d^2 - R^2}}$ is the cell area. By Theorem 2, there exists $p = p_c^{sp} \geq \frac{2}{3}$, and therefore we obtain $1 - e^{-A} \geq \frac{2}{3} \Rightarrow$

$$\begin{aligned} R_c^{stp}(d, r) &\geq \sqrt{\frac{d^2}{1 + \frac{4r^4}{\log 3^2}}}, \\ d_c^{stp}(R, r) &\leq \sqrt{\frac{4r^4 R^2}{\log 3^2} + R^2}, \\ r_c^{stp}(d, R) &\geq \sqrt{\frac{\log 3 \sqrt{d^2 - R^2}}{2R}}. \end{aligned} \quad (19)$$

To verify with simulation, we plot the upper and lower bounds of Theorem 2 in Figure 13 (the communication range r and the spread angle α are normalized when using Equation (15)) and the empirical results from Figure 11, which are within the bounds.

6 PERFORMANCE EVALUATION

In this section, we present the numerical results to evaluate the performance of the proposed LIPS. A case study in a section of the Great Wall (i.e., Shabadun) is given to evaluate our routing methods. And we take an outdoor testbed to evaluate the performance of LIPS compared to GeRaf.

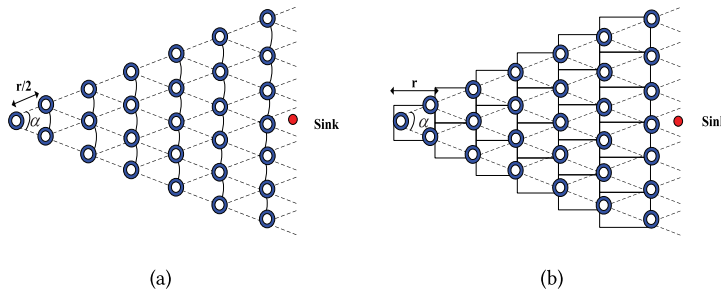


Fig. 12. Two mapping types of directed site percolation models. (a) DU is defined by a cell with a sector of angle α and radius $r/2$. (b) DL is defined by a cell with a rectangle of width r .

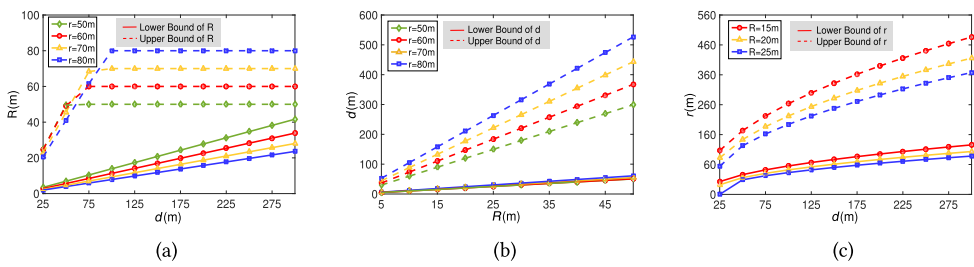


Fig. 13. The thresholds of R , d , and r . In (a), the solid lines are the lower bounds for R from Theorem 2, whereas the dashed lines are the upper bounds for R . Similarly, the bounds for d and r are in (b) and (c), respectively. Furthermore, it is clear that the simulation results are within the theoretical bounds.

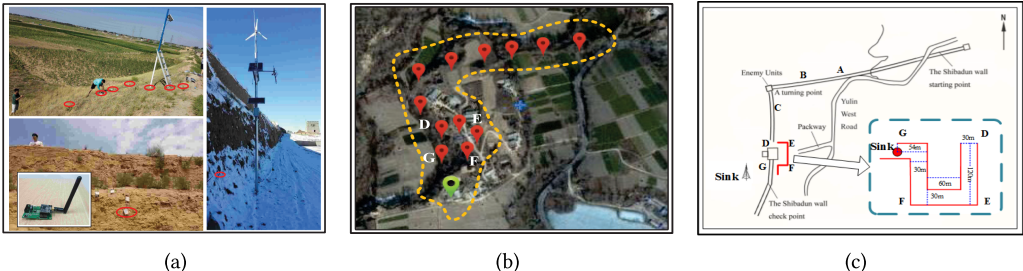


Fig. 14. Deployment. (a) Partial deployment area in Shibadun. (b) The considered monitoring area around Shibadun of the Great Wall, which continues from the southwest to the northeast of Yulin City, China. (c) The map of the portion of the Great Wall, where the area DEFG is abstracted as a monitoring region that has three turning points and the measurement of the area is shown clearly.

6.1 Deployment in Shibadun

In this work, we conduct a measurement study on Shibadun, a part of the Great Wall, which is a long-term and multi-year sensor network deployment for Great Wall monitoring. With up to 100 nodes deployed in the wild, Shibadun provides us an excellent platform for employing our LIPS. Figure 14(a) shows the partial real deployment in Shibadun.

6.2 Simulation Setup

In Great Wall monitoring, the monitoring region often presents a complicated strip structure. For example, a critical monitoring area around Shibadun of the Great Wall is shown in Figure 14(b),

which continues from the southwest to the northeast of Yulin City. From the area $DEFG$, we can abstract a monitoring region that has three turning points, and the size of the area is shown in Figure 14(c). Packets have to be forwarded along the strip structure hop by hop to the sink, and the path from the source node to the sink node consists of a strip topology with turning points.

In this simulation, the width of the strip network is 30m and the total length is 324m, as shown in Figure 14(c). The transmission power of each node is 0 dB. The sink node is fixed at the upper left corner, and other nodes locations are randomly assigned. Extensive situations are examined by varying communication ranges and node densities. In each setting, we performed 100 independent runs, with 2,000 packets sent in each run. In the following, each result in the Figure is the average value of the 100 runs. We use ZigBee as the underlying protocol. The channel model and an energy consumption model are as follows.

Channel model. To simulate a realistic channel model for the WSN, we use the log-normal shadowing path loss model derived in Srinivasa and Haenggi [25] because this model considers the path-loss exponent and log-normal shadowing variance of the environment, and the modulation and encoding schemes of the radio.

Energy consumption model. Here we use the same energy consumption model as in Heinzelman et al. [9]. The energy consumptions for transmitting (E_{tx}) or receiving (E_{rx}) b bits are calculated as follows:

$$E_{tx} = E_e \times b + \epsilon \times b \times r^\alpha, \quad (20)$$

$$E_{rx} = E_e \times b, \quad (21)$$

where E_e is the energy consumption for transmission circuit or reception circuit, and ϵ is the amplifier parameter of amplifier power. α is the attenuation of the path. According to the existing work, the energy consumption of idle listening is approximately equal to the receiving consumption, and thus we set $E_{idle} = E_{rx}$ in our simulation. The total energy consumption of node i can be expressed as

$$E_{con} = E_{tx} + E_{rx} + E_{idle}. \quad (22)$$

6.3 Evaluation Metrics

We compare LIPS against the following routing protocols:

- *Geographic based:* (i) GeRaf [30], a traditional GOR algorithm that assigns the forwarders that are closer to the destination with higher relay priorities, and (ii) GLIDER[21], an improved algorithm that decomposes the network into pieces and uses simple GredR inside each piece. Unlike GeRaf, GLIDER can achieve high transmission success rate especially in the network with holes.
- *Greedy based:* Homotopic routing [11] generates constant bounded stretch compared to the shortest path, which can provide the low cost of delay.

To gain a deep understanding of the performance of LIPS, we first compare it to GeRaf to evaluate whether it can improve the transmission success rate when used in the SNWT. We also compare LIPS with GLIDER and homotopic routing to evaluate whether it can provide a short path and reduce the costs of both the energy and the communication. To do so, we define the evaluation metrics as shown in Table 2.

6.4 Performance Comparison

6.4.1 Transmission Success Rate of LIPS. In this simulation, we modified the forwarding priority mechanism in GeRaf [30]. Instead of choosing the forwarder that is closer to the sink having higher

Table 2. List of Performance Metrics

Metrics	Definition
Transmission success rate	Measured in the ratio of the number of successful transmissions and total transmissions.
Total number of packet exchange	Measured by the ratio of the total energy cost and the total initial energy in the whole network.
Energy consumption rate	Measured by the ratio of the total cost energy and the total initial energy during the network-wide. The receiver-side energy is determined by their predefined working schedules, which are not changed by designs. Therefore, we use only the sender-side energy as the performance metric when we compare different designs under the same duty-cycled schedules.
Path length	Measured by the total hops from one source node to sink if the packet is transmitted successfully.

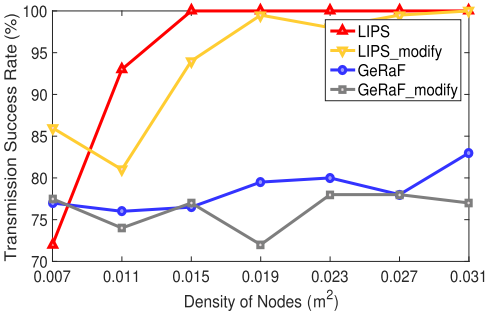
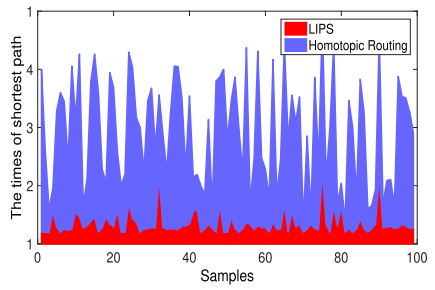
Fig. 15. Transmission success rate under different ρ .

Fig. 16. Comparison of path length.

forwarding priorities, we select a node randomly as the forwarder in the candidate set and define it as GeRaF_modify. We aim to test the transmission success rate of LIPS, LIPS_modify, GeRaF, and GeRaF_modify. The communication range r is set to 40m, and the parameter R is set to 20m according to the analysis in Section 5. Then we evaluate the impact of the node density ρ on the routing performance, and we increase the node density from $0.007/m^2$ to $0.031/m^2$ with step $0.004/m^2$. Each result is averaged over 1,000 runs.

The transmission success rate is illustrated in Figure 15. Clearly, LIPS outperforms GeRaF. LIPS achieves a nearly 100% transmission success rate. This translates to a 20% improvement when compared to the 80% transmission success rate achieved by GeRaF when the density changes from $0.015/m^2$ to $0.031/m^2$ since GeRaF does not involve transmission direction when choosing the candidate set. Interestingly, we find that modified algorithms have lower probability, because they choose the forwarders randomly without considering the geographic information. They are the baseline of the comparison. However, when the node density is 0.007, the successful rate of LIPS is 72% whereas GeRaF is 77%. That means our algorithm outperforms the GeRaF when the nodes are relatively dense deployed. However, if the node density is sparse, GeRaF also cannot achieve a higher successful rate (e.g., 70%). Figure 17 further illustrates the locations of the routing failure nodes. In the GeRaF algorithm, most routing failure nodes are located in the third region because it only assigns the forwarders that are closer to sink with higher relay priorities and does not

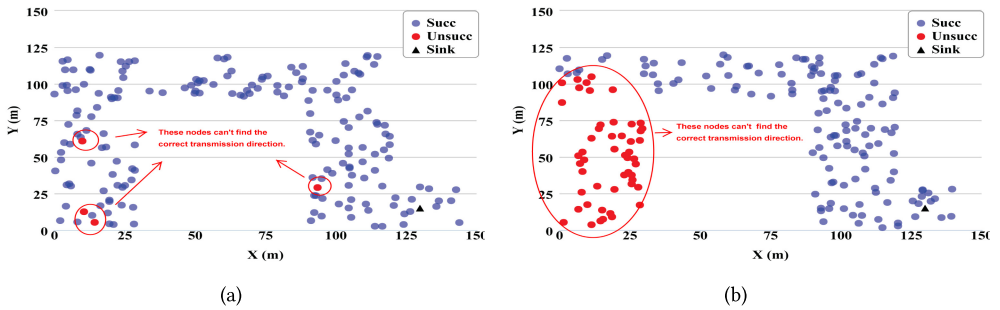
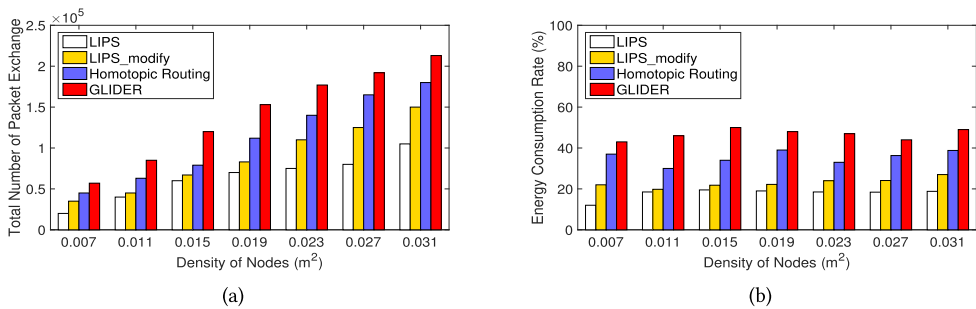


Fig. 17. (a) Transmission node of LIPS. (b) Transmission node of GeRaf.

Fig. 18. Total number of the packet exchange and energy consumption ratio under different ρ .

consider the transmission direction. In contrast, there are only a few routing failure nodes that are caused by link quality randomly distributed in the region since LIPS uses the VPM to ensure the transmission direction.

6.4.2 Costs of the Energy and the Communication of LIPS. In this simulation, we are aiming at comparing LIPS to GLIDER and homotopic routing to evaluate the costs of the energy and the communication. As shown in Figure 18(a), the total number of package exchanges of the four algorithms increases with the increasing of node density. We observe that both homotopic routing and GLIDER are higher than LIPS since they have to divide the whole network into the triangles or polygons, which causes more communication costs. The energy consumption rate is plotted in Figure 18(b). There is no obvious fluctuation of four algorithms when increasing the node density. However, the other algorithms are also higher compared to LIPS, which is consistent with the total number of package exchange because more communication results in more energy. On average, the communication overhead and energy consumption rate are 33.11% and 40.23% lower compared to the state-of-the-art algorithms. These results suggest that our solution presents the better performance, especially in the complicated strip networks.

6.4.3 Delay of LIPS. Furthermore, we compare the path length of LIPS to the homotopic routing algorithm. We choose the shortest path as the baseline and compare LIPS and homotopic routing to it, respectively. In this simulation, we randomly choose 100 source nodes and compare their path length. Figure 16 shows the results. It is obvious that LIPS can provide a path that is close to the shortest one, whereas homotopic routing is much longer than the shortest path.

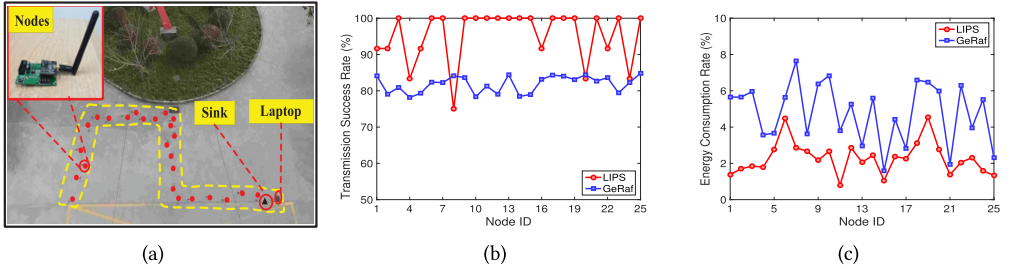


Fig. 19. Real experiment scenario and results of the transmission success rate and energy consumption.

Downloaded from the ACM Digital Library by Xidian University on April 7, 2025.

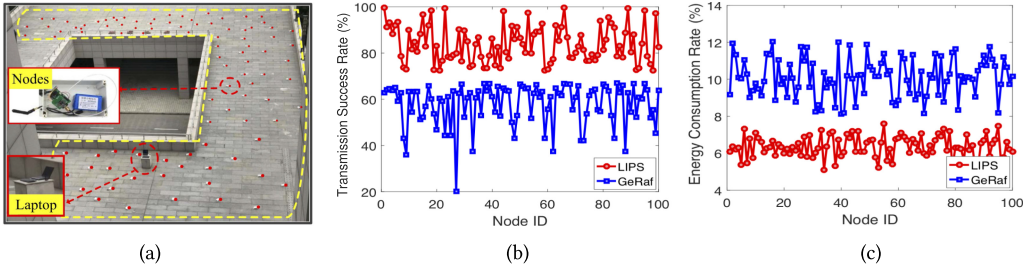


Fig. 20. (a) The outdoor scenario with 100-node testbed. Results of the transmission success rate (b) and energy consumption (c).

6.5 Experiment

In this section, we conduct an outdoor testbed shown in Figure 19(a) to verify the transmission success rate and energy consumption in turning points of LIPS compared to the GOR-based method.

6.5.1 Transmission Success Rate. We use the transmission success rate to measure the quantity of the received data. The transmission success rate is defined as the ratio of the number of packets received by the sink by the total number of packets sent by all nodes. The packet loss is defined as 1 minus the transmission success rate.

Figure 19(a) shows the real scenario with 25 nodes. The sink is deployed at the lower right corner. This experiment lasted for 4 hours, and the data sending rate of each node is three packets per hour. Our main comparison metrics are the transmission success rate and energy cost of LIPS and the GOR-based technique. Figure 19(b) illustrates the test results of the transmission success rate. As we can see, the transmission success rate of LIPS is between 90% and 100%, whereas GeRaf is 80% on average.

6.5.2 Energy Consumption. We use the energy consumption rate to measure the energy consumption. The energy consumption rate is defined as 1 minus the ratio of the residual energy at the end of the 3 testing days by initial energy at the beginning.

In Figure 19(c), we plot the statistics of how 25 nodes consumed energy for a period of 4 hours. The energy consumption rate of each node in LIPS is lower than that of GeRaf.

6.5.3 100 Nodes Testbed Evaluation. We conduct an outdoor testbed experiment with 100 nodes shown in Figure 20(a) to evaluate the transmission performance of LIPS under a strip network with multiple turning points. As the Figure shows, 100 nodes were randomly deployed within the dotted yellow line on the roof of the platform with the size of 60×100 m. There are two turning points in this monitoring area, and the sink node was located at the lower right corner. Due to the side

effect of the ground on the wireless signal propagation, the longest communication range can only reach 20m in this real experiment. The data sending rate of each node is two packets per hour, and the experiment lasted for 3 days. During our experiment, there were no people present on the roof of the building, and there were no birds or other animals either since the location of our university is far from nature. In addition, it was sunny during the experiment, so our nodes were protected very well.

Figure 20(b) shows the comparison of the transmission success rate of each node between the proposed LIPS and GeRaf algorithm. Obviously, LIPS has the higher transmission success rate because LIPS can solve the packets loss problem in the turning area by mapping the node's location to its virtual image location and eliminate the side effect of this turning area. The average success rate of LIPS and GeRaf are 83.94% and 57.96%, respectively. Compared to the 25-node testbed, the average transmission success rate of LIPS is reduced from 94.88% to 83.94%. This is reasonable because when the size of the monitoring area becomes larger, the number of hops will increase accordingly, which will eventually increase the packets loss rate. Nevertheless, the proposed LIPS still can improve the transmission success rate up to 25.98% compared to the existing work under a 100-node testbed.

Figure 20(c) shows the energy consumption of 100 nodes in the preceding experiment. From this Figure, we can see that the energy consumption rate of each node presents random fluctuation and LIPS has lower energy consumption compared to GeRaf. The average consumption rates of LISP and GeRaf are 6.82% and 11.03%.

6.6 Discussion

6.6.1 The VPM Algorithm. There are a few points are worth noting when using the VPM algorithm:

- According to the preceding analysis, the VPM algorithm can exactly provide a short path that can map a given strip network structure into the straight. Furthermore, it is obvious that the nodes in front of the virtual mirror are used to forward data frequently, whereas others behind the virtual mirror are never used. To achieve the load balance, we can take advantage of this when deploying WSN nodes at the turning area of the strip network. For example, no sensor node is needed to be deployed on the back side of the virtual mirror if connectivity is our only concern. It can also save the cost of deployment.
- Unlike other GR schemes where the topology of the network must be known by each sensor node, only the locations of the sink node and the virtual mirror are needed by each sensor node. This significantly reduces the amount of information needed at each node, and this is considered to be an advantage for the resource-restricted sensors. Additionally, the VPM algorithm generates constant bounded stretch compared to the shortest path, which will be proved in the next section.

6.6.2 Discussions in Non-Strip Networks. In this section, we will discuss whether LIPS can be used in non-strip networks, just as in the ideal scenario, such as a square region. We simulate a square network with side length l , where N sensor nodes are randomly deployed. Then we change the node number N and parameter R to evaluate LIPS compared to GeRaf. A further evaluation of the impact of R is provided. Finally, we discuss the scalability of LIPS.

1. The impact of the total number N of nodes.

We compare the performance under different node density. For different density, we change the number of the total sensors while fixing the size of the monitoring region. The total number of packet exchange is plotted in Figure 21(a). We observe that the packet

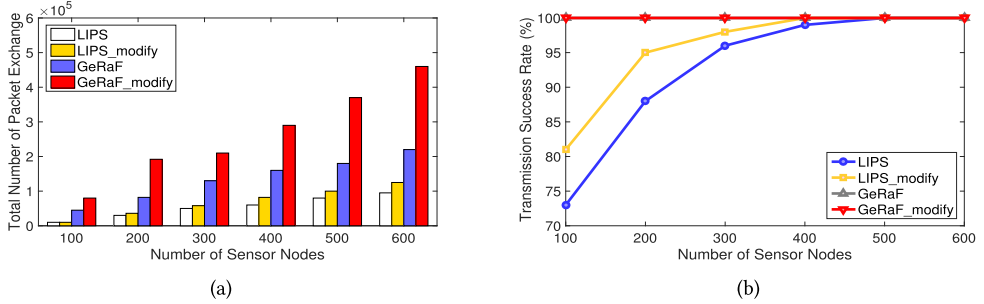


Fig. 21. (a) Number of packet exchange under different N . (b) Transmission success rate under different N .

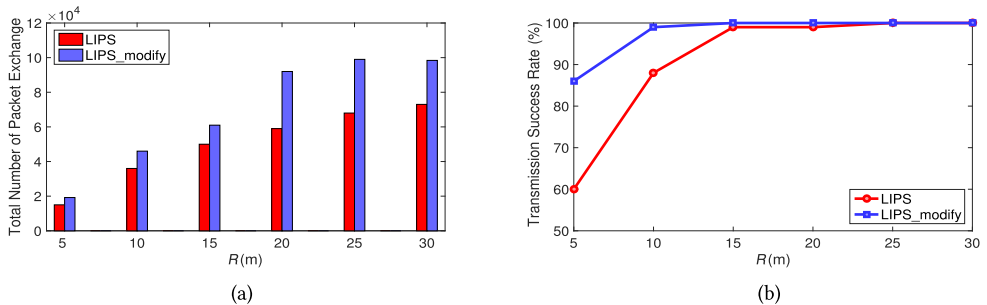


Fig. 22. (a) Number of packet exchange under different R . (b) Transmission success rate under different R .

exchange of GeRaF and GeRaF_modify grow quickly when N increases, whereas LIPS and LIPS_modify just exhibit a slow growth. From Figure 21(b), it is clear that the transmission success rate increases as N increase. We analyze the reason and realize that a higher node density will obtain more candidates in the spread angle to build a transmission path with higher probability.

2. The impact of the parameter R .

In the forwarding candidates selection algorithm VPM, we use the parameter R to correct the transmission angle that represents the tradeoff between the transmission success rate and communication cost. This section addresses how parameter R affects the routing performance. Figure 22 plots the total number of packet exchange and the transmission success rate, respectively. As R increases, the total number of packet exchange becomes higher and more nodes are included in the candidate set, leading to more opportunistic forwarding and communication overhead. However, the transmission success rate is close to one when R is increased. Thus, the proper range of R is larger than 15m but still smaller than r . This result keeps consistent with theoretic proof in Section 5.

Based on all the comparisons, we conclude that LIPS outperforms the traditional GOR. More specifically, LIPS significantly saves energy and communication cost but only needs a few bytes to store the information of virtual mirrors. Furthermore, we observe more performance improvement from LIPS as compared to previous state-of-the-art algorithms in both strip network structures and ideal scenarios.

3. The key parameters in LIPS.

Localization cost. Compared to other non-GOR, our solution LIPS needs nodes' location information, which is also the case for traditional GOR. However, in the application of

Great Wall monitoring, the localization is a one-time process since the nodes are never moved after deployed.

What is the proper value of parameter R? Given a distance from the source node to sink, the value of parameter R indicates the spread angle α of transmission direction. Specifically, $\sin \alpha/2 = \frac{R}{d}$. Supposing that R is large enough, there may be more candidates within the angle. However, if R is too small, there will be not any candidate to forward the data. Thus, R should be set according to a different network configuration. That means that it can meet different design requirements by choosing a proper value. In the future, we will try to fix the spread angle α instead of the parameter R in a given network configuration.

4. *The scalability of LIPS.*

Although we designed LIPS for a strip network, the basic idea can be extended to more general scenarios, such as loop structure. During the initial stage of LIPS, we apply the approximate convex decomposition [18] method to identify the boundary node, then based on the relative locations between these boundary nodes, we established the relative coordinate for each node in the monitoring area. Thus, the loop structure can be identified in the initial stage. After that, we can divide the loop structure into two independent parts based on the location of sink node. Then each part has its own sequence of virtual mirrors. Accordingly, each node can transmit packets along its own virtual mirrors. For the more complicated loop structures, we leave it to our future work.

6.6.3 Discussion in Limitations. As illustrated earlier, LIPS has a very different candidates selection from most existing GOR algorithms. Instead of choosing the candidates only by considering the geography information, LIPS selects the candidates according to the deployed structures for strip network scenarios, which inevitably bring about several limitations. First, the strip structure cannot be mapped to a straight one without known deployed structures (e.g., the width, the length, the number of turning points, and each turning angle of the strip network are known to us). This may cause a scalability problem as the size of the monitoring area could be very larger. Second, LIPS has some other specific requirements—for example, the VPM algorithm assumes that each node knows its own location information and together with its neighbors and the sink (destination). In situations where such information is not known, the performance, especially transmission success rate, of LIPS is likely to be adversely affected.

7 CONCLUSION

Monitoring applications, such as Great Wall monitoring applications, are deploying numerous sensor nodes to improve data transmission efficiency. A common complaint they have about the routing strategy is the lack of a low-cost solution to the strip network's complexity. The classic GredR strategies would cause a significant amount of energy consumption for complicated strip structure. The traditional GOR works address geographic information of sensor nodes without considering the direction of the transmitting path. That causes packet loss and fails to handle some special cases in strip network structures. However, in many monitoring applications, the deployment environment often includes a strip structure, such as pipeline monitoring and vehicle monitoring. In light of this, we have designed a new OR algorithm, LIPS, for the strip network structures. We show through theoretical analysis and extensive simulations that our solution, VPM, provides the validity and efficiency of candidates selection in the strip network. Furthermore, LIPS can harvest more performance improvement no matter if in the strip network structures or in the non-strip scenarios. Compared to the classic algorithm, LIPS improves the transmission success rate up by 26.37%, and reduces the communication overhead down by 33.11% and the energy consumption rate down by 40.23%. Meanwhile, the length of the path in LIPS is two times the length of the shortest path.

REFERENCES

- [1] Sanjit Biswas and Robert Morris. 2004. Opportunistic routing in multi-hop wireless networks. *ACM SIGCOMM Computer Communication Review* 34, 1 (2004), 69–74.
- [2] Chi-Kin Chau, Richard J. Gibbens, and Don Towsley. 2012. Impact of directional transmission in large-scale multi-hop wireless ad hoc networks. In *Proceedings of IEEE INFOCOM (INFOCOM'12)*. IEEE, Los Alamitos, CA, 522–530.
- [3] Dezun Dong, Yunhao Liu, and Xiangke Liao. 2009. Fine-grained boundary recognition in wireless ad hoc and sensor networks by topological methods. In *Proceedings of the 10th ACM International Symposium on Mobile Ad Hoc Networking and Computing*. ACM, New York, NY, 135–144.
- [4] R. Wattenhofer, F. Kuhn, and A. Zollinger. 2003. Worst-case optimal and average-case efficient geometric ad-hoc routing. In *Proceedings of the 4th ACM International Symposium on Mobile Ad Hoc Networking and Computing (MobiHoc'03)*. ACM, New York, NY, 267–278.
- [5] Holger Füßler, Jörg Widmer, Michael Käsemann, Martin Mauve, and Hannes Hartenstein. 2003. Contention-based forwarding for mobile ad hoc networks. *Ad Hoc Networks* 1, 4 (2003), 351–369.
- [6] Geoffrey Grimmett and Philipp Hiemer. 2002. Directed percolation and random walk. In *In and Out of Equilibrium*. Springer, 273–297.
- [7] L. Guo, R. Beyah, and Y. Li. 2011. SMITE: A stochastic compressive data collection protocol for mobile wireless sensor networks. In *Proceedings of IEEE INFOCOM (INFOCOM'11)*. Los Alamitos, CA, 1611–1619.
- [8] Y. Guo, F. Kong, D. Zhu, A. Tosun, and D. Quingxu. 2010. Sensor placement for lifetime maximization in monitoring oil pipeline. In *Proceedings of the 1st ACM/IEEE International Conference on Cyber-Physical Systems*. 61–68.
- [9] Wendi B. Heinzelman, Anantha P. Chandrakasan, and Hari Balakrishnan. 2002. An application-specific protocol architecture for wireless microsensor networks. *IEEE Transactions on Wireless Communications* 1, 4 (2002), 660–670.
- [10] I. Jawhar, N. Mohamed, M. M. Mohamed, and J. Aziz. 2008. A routing protocol and addressing scheme for oil, gas, and water pipeline monitoring using wireless sensor networks. In *Proceedings of the IFIP International Conference on Wireless and Optical Communications Networks*. 1–5.
- [11] K. Huang, C.-C. Ni, R. Sarkar, J. Gao, and J. S. B. Mitchell. 2014. Bounded stretch geographic homotopic routing in sensor networks. In *Proceedings of IEEE INFOCOM (INFOCOM'14)*. IEEE, Los Alamitos, CA, 979–987.
- [12] Fabian Kuhn, Roger Wattenhofer, Yan Zhang, and Aaron Zollinger. 2003. Geometric ad-hoc routing: Of theory and practice. In *Proceedings of the 22nd Annual Symposium on Principles of Distributed Computing (PODC'03)*. ACM, New York, NY, 63–72.
- [13] Seungjoon Lee, Bobby Bhattacharjee, and Suman Banerjee. 2005. Efficient geographic routing in multihop wireless networks. In *Proceedings of the 6th ACM International Symposium on Mobile Ad Hoc Networking and Computing (MobiHoc'05)*. ACM, New York, NY, 230–241.
- [14] Uichin Lee, Biao Zhou, Mario Gerla, Eugenio Magistretti, Paolo Bellavista, and Antonio Corradi. 2006. Mobeyes: Smart mobs for urban monitoring with a vehicular sensor network. *IEEE Wireless Communications* 13, 5 (2006), 52–57.
- [15] Thomas M. Liggett. 1995. Survival of discrete time growth models, with applications to oriented percolation. *Annals of Applied Probability* 5, 3 (1995), 613–636.
- [16] Chen Liu, Xiaojiang Chen, Dingyi Fang, Dan Xu, Zhanyong Tang, and Chieh Jan Mike Liang. 2015. LIPS: Bring Light Propagation Selection to geographic opportunistic routing in strip WSNs. In *Proceedings of the Workshop on Mobile Sensing*. 39–44.
- [17] Wenping Liu, Hongbo Jiang, Yang Yang, Xiaofei Liao, Hongzhi Lin, and Zemeng Jin. 2015. A unified framework for line-like skeleton extraction in 2D/3D sensor networks. *IEEE Transactions on Computers* 64, 5 (2015), 1323–1335.
- [18] Wenping Liu, Dan Wang, Hongbo Jiang, Wenyu Liu, and Chonggang Wang. 2015. An approximate convex decomposition protocol for wireless sensor network localization in arbitrary-shaped fields. *IEEE Transactions on Parallel and Distributed Systems* 26, 12 (2015), 3264–3274.
- [19] B. O'Flynn, R. Martinez, J. Cleary, C. Slater, F. Regan, D. Diamond, and H. Murphy. 2007. SmartCoast: A wireless sensor network for water quality monitoring. In *Proceedings of the 32nd IEEE Conference on Local Computer Networks (LCN'07)*. IEEE, Los Alamitos, CA, 815–816.
- [20] C. E. M. Pearce and F. K. Fletcher. 2005. Oriented site percolation, phase transitions and probability bounds. *Journal of Inequalities in Pure and Applied Mathematics* 6, 5 (2005), Article 135, 15 pp.
- [21] L. Guibas V. de Silva Q. Fang, J. Gao, and L. Zhang. 2005. GLIDER: Gradient landmark-based distributed routing for sensor networks. In *Proceedings of IEEE INFOCOM (INFOCOM'05)*, Vol. 1. IEEE, Los Alamitos, CA, 339–350.
- [22] Karim Seada, Marco Zuniga, Ahmed Helmy, and Bhaskar Krishnamachari. 2004. Energy-efficient forwarding strategies for geographic routing in lossy wireless sensor networks. In *Proceedings of the 2nd International Conference on Embedded Networked Sensor Systems (SenSys'04)*. ACM, New York, NY, 108–121.
- [23] R. C. Shah, A. Bonivento, D. Petrovic, E. Lin, J. Van Greunen, and J. Rabaey. 2004. Joint optimization of a protocol stack for sensor networks. In *Proceedings of the Military Communications Conference (MILCOM'04)*, Vol. 1. IEEE, Los Alamitos, CA, 480–486.

- [24] R. C. Shah and J. M. Rabaey. 2002. Energy aware routing for low energy ad hoc sensor networks. In *Proceedings of the 2002 Wireless Communications and Networking Conference (WCNC'02)*, Vol. 1. 350–355.
- [25] S. Srinivasa and M. Haenggi. 2009. Path loss exponent estimation in large wireless networks. In *Proceedings of the Information Theory and Applications Workshop*. 738–752.
- [26] I. Stoianov, L. Nachman, S. Madden, T. Tokmouline, and M. Csail. 2007. PIPENET: A wireless sensor network for pipeline monitoring. In *Proceedings of the 2007 6th International Symposium on Information Processing in Sensor Networks (IPSN'07)*. IEEE, Los Alamitos, CA, 264–273.
- [27] Guang Tan, Hongbo Jiang, Jun Liu, and Anne-Marie Kermarrec. 2014. Convex partitioning of large-scale sensor networks in complex fields: Algorithms and applications. *ACM Transactions on Sensor Networks* 10, 3 (2014), 41.
- [28] Kai Zeng, Jie Yang, and Wenjing Lou. 2012. On energy efficiency of geographic opportunistic routing in lossy multihop wireless networks. *Wireless Networks* 18, 8 (2012), 967–983.
- [29] Kai Zeng, Zhenyu Yang, and Wenjing Lou. 2009. Location-aided opportunistic forwarding in multirate and multihop wireless networks. *IEEE Transactions on Vehicular Technology* 58, 6 (2009), 3032–3040.
- [30] Michele Zorzi and Ramesh R. Rao. 2003. Geographic random forwarding (GeRaF) for ad hoc and sensor networks: Energy and latency performance. *IEEE Transactions on Mobile Computing* 2, 4 (2003), 349–365.

Received August 2017; revised May 2018; accepted January 2019